Molecular Simulation

ISSN: 0892-7022 (Print) 1029-0435 (Online) Journal homepage: https://www.tandfonline.com/loi/gmos20

Surface tension and vapour–liquid phase coexistence of variable-range hard-core attractive Yukawa fluids

Jayant K. Singh

To cite this article: Jayant K. Singh (2009) Surface tension and vapour–liquid phase coexistence of variable-range hard-core attractive Yukawa fluids, Molecular Simulation, 35:10-11, 880-887, DOI: 10.1080/08927020902787796

To link to this article: https://doi.org/10.1080/08927020902787796

Published online: 14 Aug 2009.

Molecular Simulation
Vol. 35, Nos. 10–11, September 2009, 880–887

Taylor & Francis
Taylor & Francis Group

Surface tension and vapour–liquid phase coexistence of variable-range hard-core attractive Yukawa fluids

Jayant K. Singh*

Department of Chemical Engineering, Indian Institute of Technology Kanpur, Kanpur 208016, India

(*Received 14 December 2008; final version received 25 January 2009*)

The vapour–liquid phase coexistence and surface tension of hard-core Yukawa fluids with short attraction range, $\lambda = 8.0$, 9.0 and 10.0, are reported using grand-canonical transition-matrix Monte Carlo (GC-TMMC) with the histogram reweighting method. Surface tension is calculated using finite-size scaling approach of Binder. We also compare GC-TMMC results with the available literature data for Yukawa fluids with $\lambda = 1.8$, 3.0 and 4.0. Critical properties obtained from rectilinear diameter approach and least square-technique are also reported. GC-TMMC results are found to be more precise than the previous reported values. We also present the corresponding state of surface tension for extremely short-range attractive Yukawa fluids.

Keywords: Yukawa fluids; surface tension; molecular simulation

1. Introduction

In recent years, phase transition for colloidal suspensions has become a subject of growing interest as it is commonly found in many industrial products such paints, inks, food, detergents and cosmetics. Furthermore, it plays an important role in biology, for example, blood. Interaction range of colloidal solvent can be modified by an addition of charged nanoparticles [1,2], non-adsorbing polymer [3] or other solutes [4,5]. Yukawa potential is one of the most suitable models for such systems since, upon varying the interaction range, one can represent the behaviour of some real system. Moreover, its analytical tractability adds to its popularity as a simple model for protein liquids [6,7], charged stabilised colloids [8] and ionic fluids [9,10]. Yukawa potential is represented by the following expression:

$$u(r) = \begin{cases} \infty & \text{if } r < \sigma \\ -\frac{\varepsilon\sigma}{r}\exp\left(-\lambda(r-\sigma)\right) & \text{if } r \geq \sigma \end{cases}, \qquad (1)$$

where ε is the potential depth, σ is the molecular diameter and λ is the range of the potential.

Vapour–liquid equilibria of Yukawa potential has been studied by a few authors recently by various theoretical approaches [6,7,11–13]. Furthermore, this was aided by molecular simulation studies on the same model system [4,14,15]. The molecular simulation techniques mainly used by earlier workers were based on Gibbs ensemble Monte Carlo (GEMC) [16–19] and slab-based molecular dynamics (MD) and Monte Carlo (MC) methods [14,20,21]. The results of the former method yield coexistence properties of the bulk phase without the contact of the phases; hence GEMC is unable to capture interfacial properties. On the other hand, the latter method is mainly popular to obtain interfacial properties but requires a larger system size for the stabilisation of the vapour–liquid interface. Moreover, such a method is not suitable at higher temperature for the evaluation of bulk properties compared with other available methods [22]. The other prominent approaches for the study of vapour–liquid equilibrium by molecular simulation include grand-canonical transition-matrix Monte Carlo [23,24], Gibbs–Duhem integration [25], and NPT + test particle [26–28]. Grand-canonical transition-matrix Monte Carlo (GC-TMMC) stands out among all the above methods due to its ability accurates to obtain phase equilibria and interfacial properties in conjunction with the finite-size scaling approach of Binder [29]. Due to its greater efficiency than GEMC and its parallelisation ability, it has been applied to a variety of systems [30–35].

Molecular simulation data for vapour–liquid interfacial properties of Yukawa fluids are scarce. Moreover, there is a lack of agreement in the data available in the literature, which is based on either slab-based MC or MD techniques. In particular, phase coexistence and surface tension for HCAY fluid with short interaction range is not studied in details via computer simulations. Most of the molecular simulation studies until now have been done with $1.8 \leq \lambda \leq 7.0$. This work is primarily to provide the phase equilibria and interfacial properties of Yukawa fluids with extremely short attraction range using GC-TMMC and finite-size scaling approach [29].

*Email: jayantks@iitk.ac.in

ISSN 0892-7022 print/ISSN 1029-0435 online

DOI: 10.1080/08927020902787796
http://www.informaworld.com

Additionally, we compare the results of variable attraction range via GC-TMMC with those available in the literature.

The rest of the paper is organised as follows: in the next section, we briefly describe methods used for calculating the phase equilibria and interfacial properties by molecular simulation along with simulation details; Section 3 presents the results and discussion, and we conclude in Section 4.

2. Methodology

In this work, simulations are conducted in the grand-canonical ensemble, where the chemical potential μ, volume V and temperature T are kept fixed and particle number N and energy U fluctuate. The probability π_s of observing a microstate s with energy U_S and particle number N_S is,

$$\pi_s = \frac{1}{\Xi}\frac{V^{N_s}}{\Lambda^{3N_s}N_s!}\exp\left[-\beta(U_s - \mu N_s)\right], \tag{2}$$

where $\beta = 1/k_B T$ is the inverse temperature, Ξ is the grand-canonical partition function and Λ is the de Broglie wavelength. The probability $\Pi(N)$ of observing a macrostate with a given number of molecules (density) is given by,

$$\Pi(N) = \sum_{N_s=N}\pi_s. \tag{3}$$

We employ the transition-matrix Monte Carlo scheme [36] with an N-dependent sampling bias to obtain the probability distribution $\Pi(N)$. The method monitors the acceptance probability of attempted MC moves and subsequently uses this information to calculate the macrostate transition-probability matrix. For every attempted move from a microstate s to a microstate t, regardless of whether the move is accepted, we update a collection matrix C with the acceptance probability $a(s \to t) = \min[1, \pi_t/\pi_s]$ as follows,

$$\begin{aligned} C(N \to M) &= C(N \to M) + a(s \to t) \\ \text{and} \\ C(N \to N) &= C(N \to N) + 1 - a(s \to t), \end{aligned} \tag{4}$$

where N and M represent the macrostate labels for microstates s and t, respectively. At any time during the simulation, the macrostate transition-probability matrix can be obtained by appropriately normalising the collection matrix,

$$P(N \to M) = \frac{C(N \to M)}{\sum_O C(N \to O)}. \tag{5}$$

Macrostate probabilities are obtained by utilising the detailed balance expression,

$$\Pi(N)P(N \to M) = \Pi(M)P(M \to N).$$

For a grand-canonical simulation, where transitions in N are such that $N \to N$, $N \to N+1$ and $N \to N-1$, the transition-probability matrix P is tri-diagonal. In such conditions, a sequential approach provides a suitable means for obtaining the macrostate probabilities,

$$\ln\Pi(N+1) = \ln\Pi(N) - \ln\left[\frac{P(N+1 \to N)}{P(N \to N+1)}\right]. \tag{6}$$

To ensure adequate sampling of all states, we employ a multi-canonical sampling [37] scheme that encourages the system to sample all densities with uniform frequency. This procedure is implemented by assigning each macrostate a weight $\eta(N)$ that is inversely proportional to the current estimate of its probability, $\eta(N) = -\ln\Pi(N)$. Acceptance criteria are modified to account for the bias as follows,

$$a_\eta(s \to t) = \min\left[1, \frac{\eta(M)\pi_t}{\eta(N)\pi_s}\right], \tag{7}$$

where $\eta(N)$ and $\eta(M)$ are weights corresponding to microstates s and t, respectively. Introduction of a weighting function does not alter the mechanism through which the collection matrix is updated. The unbiased acceptance probability is still used to update the collection matrix.

Simulations are conducted at a specified value of the chemical potential, which is not necessarily close to the saturation value. To determine the phase-coexistence value of the chemical potential, the histogram reweighting method of Ferrenberg and Swendson [38] is used. This method enables one to shift the probability distribution obtained from a simulation at chemical potential μ_0 to a probability distribution corresponding to a chemical potential μ using the relation,

$$\ln\Pi(N;\mu) = \ln\Pi(N;\mu_0) + \beta(\mu - \mu_0)N. \tag{8}$$

To determine the coexistence chemical potential, we apply the above relation to find the chemical potential that produces a probability distribution $\Pi_c(N)$, where the areas under the vapour and liquid regions are equal. Saturated densities are related to the first moment of the vapour and liquid peaks of the coexistence probability distribution. To calculate the saturation pressure, we use the expression

$$\beta pV = \ln\left(\sum_N \Pi_c(N)/\Pi_c(0)\right) - \ln(2). \tag{9}$$

The critical properties are estimated from a least-square fit of the law of rectilinear diameter [39]

$$\rho^l - \rho^v = C_1\left(1 - \frac{T}{T_c}\right)^{\beta_c} + C_2\left(1 - \frac{T}{T_c}\right)^{\beta_c+\Delta}, \quad (10)$$

where ρ^l and ρ^v are the liquid and vapour densities, respectively, and C_1 and C_2 are fitting parameters. The critical exponent β_c is taken as 0.325 and $\Delta = 0.51$. The critical temperature, T_c, estimate from the above is utilised to get the critical density from the least-square fit to the following expression.

$$\frac{\rho^l + \rho^v}{2} = \rho_c + C_3(T - T_c). \quad (11)$$

Critical pressure is calculated using the least-square fitting to the following expression

$$\ln P = A + B/T, \quad (12)$$

where A and B are constants.

In this work, we adopt units such that σ and ε are unity. Reduced units used in this study are temperature $T^* = kT/\varepsilon$, density $\rho^* = \rho\sigma^3$, pressure $P^* = P\sigma^3/\varepsilon$ and surface tension $\gamma^* = \gamma\sigma^2/\varepsilon$.

Simulations for calculating saturated densities and vapour pressures are conducted using Intel Xeon dual-core dual processor servers. The MC move distribution is: 30% particle displacement, 35% particle insertion and 35% particle deletion. One of the salient features of GC-TMMC is the ability to use a multiprocessor to collect the transition matrix. In this approach, we run the simulation simultaneously on a multi-processor (in the current work we have used two quad-core processors). Each core of the processor works on a specific range of the particle number i.e. each processor has the responsibility to fill a certain range of the transition matrix. We frequently gather the transition probabilities from individual processors in the global collection matrix. Hence, weights used in the multi-canonical sampling get updated frequently.

Typical maximum molecule numbers for these simulations varied from 350 to 900 for phase-coexistence calculations. Simulation size is increased at temperature closer to critical point. In general, we have used 8–10 simulation box size for phase equilibria calculation. Four runs were performed to calculate the statistical error. Each run for phase coexistence took around 2–4 h depending on the system size. Surface tension for each temperature is calculated based on box length, $L = 10$, 12 and 14. Maximum system size for such calculation is kept around 2400–2600. The run length for each simulation run varied from 10–48 h depending on system size.

3. Results and discussions

In the first part of this section, we compare the results of GC-TMMC with that from GEMC [19] and slab-based MC and MD methods [21]. Figure 1 presents the phase-coexistence envelope for interaction range $\lambda = 1.8$. Saturated densities and pressure obtained by GC-TMMC contain less than 0.5% error. Liquid phase density data of GC-TMMC are in reasonably good agreement with the GEMC data of Shukla [19] at substantial subcritical temperatures. However, GEMC data appear to deviate significantly from GC-TMMC values at higher temperature. This may be because close to the critical temperature, GEMC is known to provide erroneous values of densities

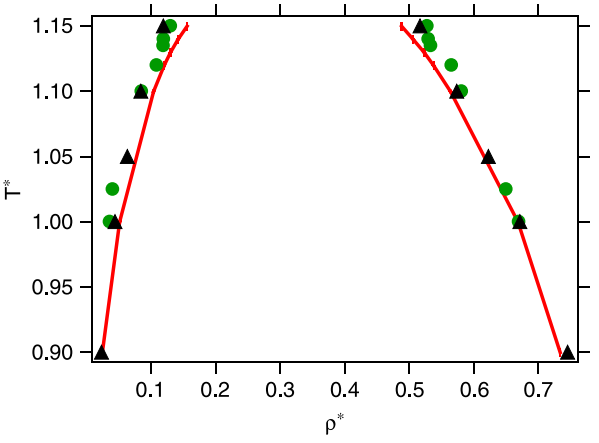

Figure 1. Coexistence vapour and liquid densities of hard-core Yukawa fluid at $\lambda = 1.8$. Solid curve represents the data obtained from GC-TMMC. Filled circles and triangles are the data from GEMC [19] and canonical Monte Carlo and molecular dynamic [21] simulations, respectively.

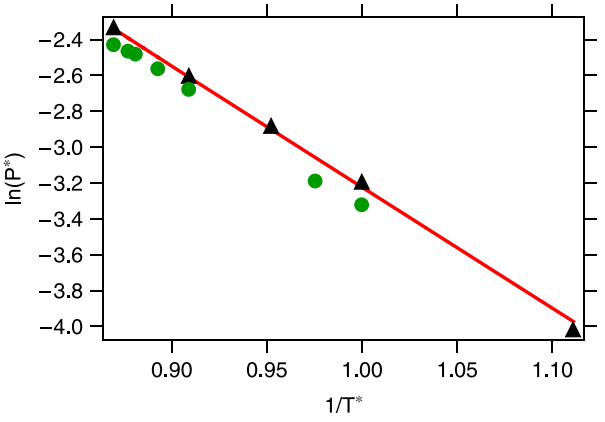

Figure 2. The vapour pressure curve of hard-core Yukawa fluid at $\lambda = 1.8$. The results of this work are shown with the other literature values. Solid line represents the data obtained from GC-TMMC. Filled circles and triangles are the data from GEMC [19] and canonical Monte Carlo and molecular dynamic [21] simulations, respectively.

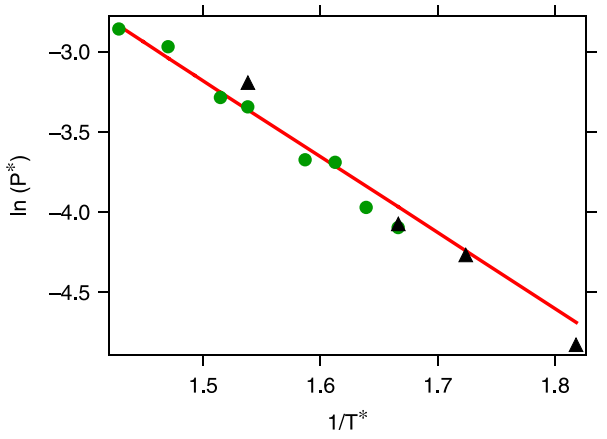

Figure 3. The vapour pressure curve of hard-core Yukawa fluid at $\lambda = 3.0$. The results of this work are shown with the other literature values. Solid line represents the data obtained from GC-TMMC. Filled triangles are the data from canonical Monte Carlo and molecular dynamic [21] simulations, respectively.

of liquid and vapour phases due to phase switch behaviour of the simulation box [40]. Moreover, system size used by Shukla for GEMC [19] appears to be insufficient for temperature closer to critical temperature. On the other hand, there is a good agreement between GC-TMMC and slab-based methods for saturated liquid density. Nevertheless, saturated vapour density due to slab-based MC and MD [21] is lower than that from GC-TMMC.

Figure 2 shows the saturated vapour pressure in a Clausius–Clapeyron plot, as calculated via GC-TMMC. Comparison with the literature data follows the same trend as with the orthobaric densities. There is in general reasonable agreement between slab-based methods and GC-TMMC; however, error associated with GEMC data is substantial. Furthermore, literature data are slightly scattered around the straight line based on the current work. Interestingly, the relative behaviour of these methods changes at lower interaction range as shown in Figure 3, which presents the vapour pressure for Yukawa fluid with $\lambda = 3.0$. It is clear that pressure calculated using GEMC simulation is in extremely good agreement; on the contrary to the case for $\lambda = 1.8$, slab-based methods yield pressure away from the GCMC simulation data. Table 1 tabulates the results for $\lambda = 1.8$, 3.0 and 4.0 via GC-TMMC.

We have used least-square technique and rectilinear diameter approach to calculate the critical points. Our estimates based on the GCMC simulations are tabulated in Table 2 along with the literature estimates. Similar to the behaviour seen in our comparison of the phase equilibrium

Table 1. Vapour–liquid coexistence data from grand-canonical transition-matrix Monte Carlo simulations of hard-core Yukawa molecules with variable interaction range ($\lambda = 1.8$, 3.0, 4.0).

λ	T^*	$\beta\mu$	P^*	ρ_v^*	ρ_l^*	γ^* (This work)	γ^* (Lit.)
1.8	0.9	-3.9829_4	0.01883_1	0.02388_2	0.7340_1		
	1.0	-3.4145_6	0.03979_3	0.05069_6	0.6686_9	0.372_1	0.37_5
							0.30_2
	1.1	-2.9878_2	0.07352_2	0.10331_5	0.5638_1	0.121_1	0.13_4
							0.09_4
	1.12	-2.9155_3	0.08211_4	0.11975_{10}	0.5378_1		
	1.13	-2.8811_2	0.08664_4	0.12971_{18}	0.5229_{11}		
	1.14	-2.8475_2	0.09136_4	0.14143_{19}	0.5058_3		
	1.15	-2.8147_3	0.09631_1	0.15545_{15}	0.4881_1	0.028_3	0.10
							0.05_1
3.0	0.55	-4.1897_{22}	0.00921_3	0.01871_6	0.8477_6	0.383_9	0.39_3
	0.58	-3.8311_8	0.01438_1	0.02905_2	0.8099_{16}		0.29_4
	0.6	-3.6184_6	0.01891_1	0.03836_3	0.7805_2		0.21_5
	0.65	-3.1718_1	0.03460_1	0.07422_1	0.6980_9	0.133_1	0.14_4
	0.66	-3.0946_2	0.03862_2	0.08463_{10}	0.6790_9		
	0.67	-3.0201_5	0.04303_3	0.09699_{10}	0.6565_{11}		
	0.68	-2.9492_1	0.04779_1	0.11167_8	0.6339_5		
	0.69	-2.8819_3	0.05292_3	0.12939_{29}	0.6070_1		
	0.70	-2.8176_2	0.05845_1	0.15244_{14}	0.5760_6		
4.0	0.45	-4.1555_{61}	0.00783_5	0.01956_{16}	0.8888_{31}		
	0.47	-3.8321_7	0.01166_1	0.02913_3	0.8633_{13}		
	0.485	-3.6166_8	0.01534_1	0.03863_6	0.8351_{10}	0.195_3	0.21_8
	0.50	-3.4193_5	0.01985_2	0.05088_6	0.8031_{16}	0.162_9	0.22_4
	0.515	-3.2403_9	0.02527_3	0.06670_{12}	0.7701_3		
	0.53	-3.0759_8	0.03179_3	0.08796_{12}	0.7306_{13}	0.0828_8	0.09_4
	0.55	-2.8792_7	0.04238_6	0.13120_{47}	0.6636_{24}		

Subscripts v and l represents vapour and liquid, respectively. The errors in densities and pressures, chemical potential and surface tension represent one SD of the mean for four independent runs. Comparison between the surface tension obtained from GC-TMMC in the present work with those of the canonical ensemble MD and MC simulations of [21].

Table 2. The critical temperature T_c^*, density ρ_c^* and pressure P_c^* data for hard-core Yukawa fluids with variable interaction range λ estimated from GC-TMMC, rectilinear diameter approach and least-square fit and compared with literature values.

λ	T_c^*	ρ_c^*	P_c^*	Source
1.8	1.180_1	0.315_1	0.110_2	This work
	1.179	0.308	0.102	[21]
	1.190	0.306	0.121	
	1.192	0.294		[18]
3.0	0.722_1	0.355_1	0.072_1	This work
	0.725	0.351	0.099	[21]
	0.715	0.375		[18]
4.0	0.572_1	0.385_1	0.057_1	This work
	0.593	0.361	0.081	[21]
	0.576	0.377		[18]
8.0	0.382_2	0.447_5	0.044_5	This work
9.0	0.362_2	0.454_5	0.043_4	This work
	0.427	0.57		[17]
10.0	0.343_2	0.471_2	0.039_1	This work

data, critical point parameters also reflect the similar scatter. For Yukawa fluid with attractive interaction range $\lambda = 1.8$, GEMC results are closer to that of GC-TMMC. Critical pressure particularly is not well predicted by the earlier workers. For example, in slab-based methods, Monte Carlo and molecular dynamics yield substantial different critical pressure. For $\lambda = 3.0$ and 4.0, the critical point predicted by the slab-based method appears erroneous.

We also compared the surface tension data calculated by GC-TMMC along with finite-size scaling technique. Figure 4 presents a typical probability distribution curve obtained for two different subcritical temperatures. Finite-size scaling for $\lambda = 1.8$ for two different temperatures as per Binder's formalism is shown in Figure 5. Table 1 summarises the surface tension results for $\lambda = 1.8$, 3.0 and 4.0. The results are in general good agreement with the slab-based methods. In general, slab-based method are efficient for surface tension calculation at lower temperature, which was also pointed out in our earlier work on square-well fluid [22]. It is evident that GC-TMMC is an excellent choice for phase equilibrium calculation as well for surface tension particularly at moderate and higher temperature; however, at significantly subcritical temperature, molecular dynamics appears to be more efficient method for interfacial property calculations.

Sampling difficulty at lower temperatures and at higher liquid densities, as observed in this work, is also common in various other systems such as polymers and associating fluids. For example, sampling of chain molecules is not efficient without utilising bias sampling techniques. Configuration bias Monte Carlo technique [41] is particular known to be extremely successful for these systems. Since its introduction, it has been applied

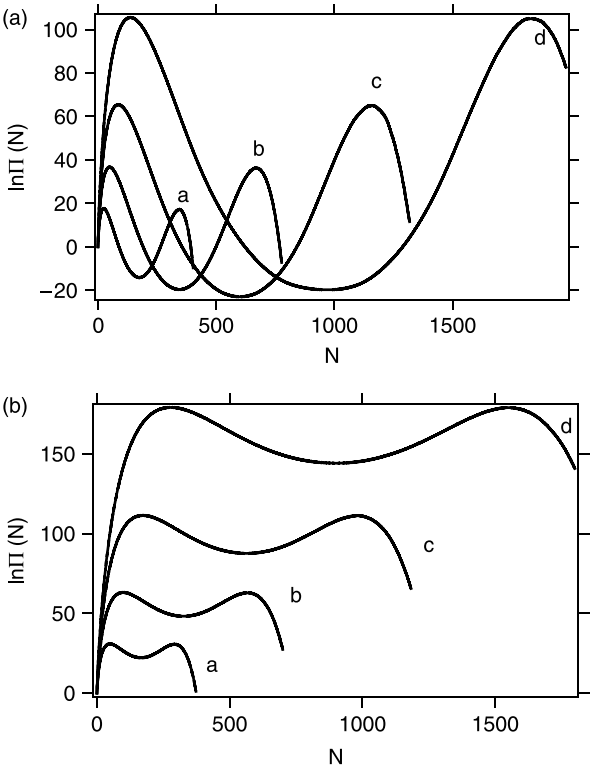

Figure 4. (a) Particle number probability distribution, for hard-core Yukawa fluid at $\lambda = 1.8$ against number of particles in the box for varying box sizes at $T* = 1.0$ at coexistence chemical potential. Curves a, b, c and d are for simulation box lengths 8, 10, 12 and 14, respectively. (b) Same as in (a) but for $T* = 1.1$.

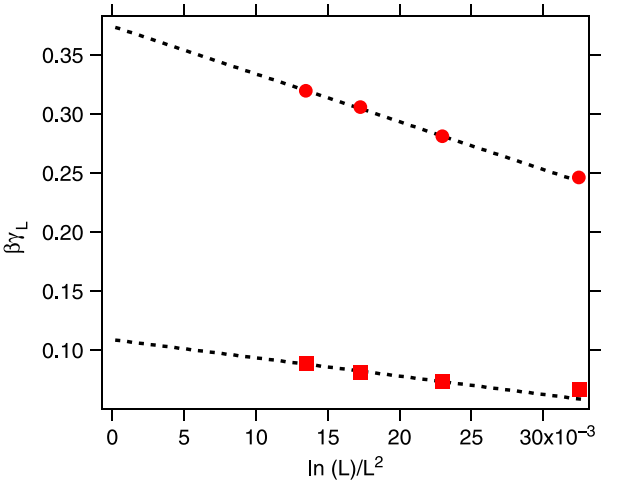

Figure 5. The system size dependence of the surface tension for hard-core Yukawa fluid with $\lambda = 1.8$ at $T* = 1.0$ and 1.1, which are represented by filled circles and squares, respectively. The dashed lines show the linear extrapolation to infinite system size. L is the edge length of the cubic simulation box.

to variety of systems [31,42]. Simulations of associating fluids, on the other hand, face a different problem. Even vapour phase of a strongly associating fluid can have local high density and it usually is a very slow relaxing system. Configurations, which are important due to favourable energy where molecules are associated, may be difficult to find through usual MC moves. Similarly, bound molecules may be rarely separated through the usual MC trials. Such problems can be remedied through the use of algorithms such as aggregation–volume bias move [43,44] or unbound–bound bias move [32,45], which have been used by many authors to alleviate sampling difficulties in associating fluids. The above methods can be combined with the GC-TMMC approach for an efficient sampling of high-density system. However, we did not employ any biasing technique apart from multi-canonical approach in this work. A thorough investigation of the sampling efficiency of GC-TMMC along with different biasing techniques for a variety of systems particularly at higher density is kept for a future study.

It is known that the range of attraction interaction determines the existence of stable vapour–liquid coexistence. Minimum attraction range should be one-sixth of the range of repulsion for stable liquid–vapour coexistence. It was shown by Dijkstra [4] that for short-range Yukawa fluid, $\lambda = 7$ and 25, fluid–fluid coexistence regions are metastable with respect to freezing. In particular, vapour–liquid equilibria data for short attractive interaction range $\lambda > 8$ are scarce for some or absent for others. Due to the metastability of fluid–fluid coexistence at extremely small interaction range, simulation is difficult to perform. Additionally, the temperature range of vapour–liquid phase transition diminishes significantly with the reduction of the attraction range and further adds to the complexity of obtaining the correct coexistence properties. We have done numerous calculations using GC-TMMC to obtain the vapour–liquid coexistence and surface tension data for $\lambda = 8.0$, 9.0 and 10.0. Table 3 summarises the data. Figure 6 presents the phase diagram of the above system. The behaviour is not much different from long interaction range systems, except that coexistence envelop is found to be smaller and shrinks with the reduction in the interaction range.

Recently, Orea and Duda [20] have worked on the corresponding states law of the Yukawa fluid. Surface tension of these fluids is found by these authors to fall on a master curve, as suggested by the corresponding state theory. On the other hand, our work as shown in Figure 7 suggests a slight variation with the range of potential, specifically for short interaction range fluids. The above

Table 3. Vapour–liquid coexistence data from GC-TMMC simulations of hard-core Yukawa molecules with variable interaction range ($\lambda = 8.0$, 9.0, 10.0).

λ	T^*	$\beta\mu$	P^*	ρ_v	ρ_l	γ
8.0	0.35	-3.1854_{11}	0.01812_1	0.0712_2	0.901_5	
	0.36	-2.9715_{11}	0.02434_5	0.1027_4	0.852_{11}	0.0498_3
	0.365	-2.8724_{18}	0.02799_8	0.1253_8	0.817_4	0.0332_{27}
	0.37	-2.7780_2	0.03212_1	0.1563_1	0.772_3	0.0188_6
	0.372	-3.2421_1	0.03389_1	0.1712_9	0.749_6	0.0135_{20}
	0.374	-3.2060_3	0.03578_2	0.1908_5	0.729_2	
	0.375	-2.6886_7	0.03676_7	0.2043_{20}	0.711_4	
9.0	0.335	-3.1075_6	0.01909_2	0.0802_1	0.906_4	
	0.34	-2.9892_{11}	0.02242_4	0.0985_3	0.870_4	
	0.345	-2.8796_5	0.02611_2	0.1215_1	0.847_1	0.0351_{25}
	0.35	-2.7746_6	0.03037_3	0.1532_7	0.800_2	
	0.351	-2.7542_5	0.03129_2	0.1622_4	0.791_3	0.0163_4
	0.352	-2.7349_8	0.03218_6	0.170_1	0.773_3	0.0143_9
	0.353	-2.7125_9	0.03332_6	0.184_2	0.759_3	
	0.354	-2.6929_{17}	0.03431_{11}	0.195_2	0.745_2	0.0075_9
	0.355	-2.6734_{13}	0.03535_{10}	0.208_2	0.726_9	
	0.356	-2.6541_{10}	0.03643_6	0.222_3	0.711_5	
	0.357	-2.6361_4	0.03744_5	0.235_2	0.699_1	
10.0	0.33	-2.8607_{10}	0.02549_3	0.1245_3	0.855_7	0.033_5
	0.331	-2.8370_{10}	0.02637_9	0.1307_8	0.846_9	
	0.332	-2.8143_8	0.02723_4	0.1375_4	0.841_4	
	0.335	-2.7455_4	0.03010_2	0.1625_6	0.799_7	0.018_2
	0.336	-2.7234_5	0.03108_3	0.1710_6	0.797_2	
	0.337	-2.7012_4	0.03212_2	0.1823_3	0.784_4	
	0.338	-2.6802_2	0.03316_1	0.1962_2	0.763_2	
	0.34	-2.6361_{13}	0.03550_{10}	0.2294_{40}	0.719_7	0.0052_8

Subscripts *v* and *l* represents vapour and liquid, respectively. The errors in densities and pressures, chemical potential and surface tension represent one SD of the mean for four independent runs.

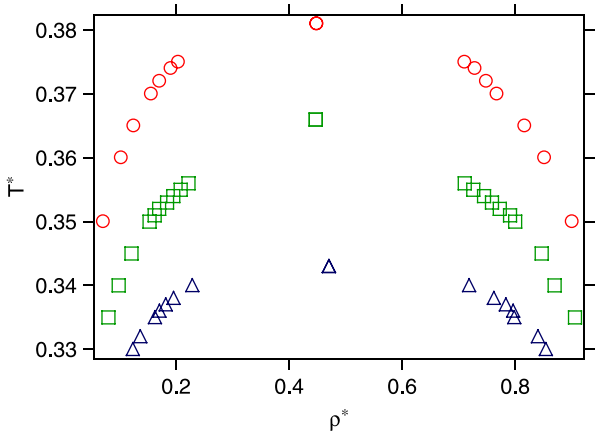

Figure 6. Coexistence vapour and liquid densities of hard-core Yukawa fluid for three values of interaction range $\lambda = 8.0$, 9.0 and 10.0. Filled symbol represent the corresponding critical point.

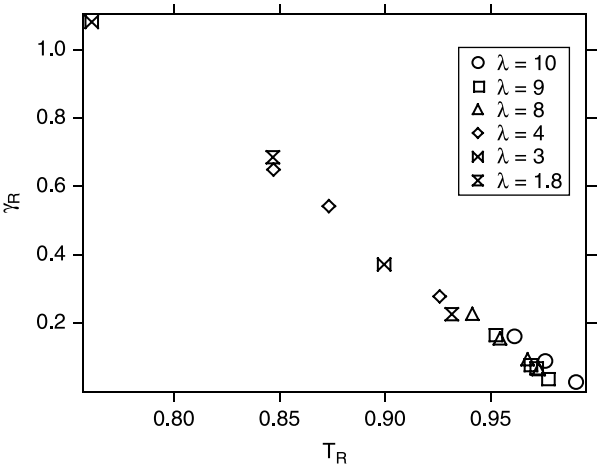

Figure 7. Reduced surface tension $\gamma_R = \gamma/(\rho^{2/3}T_c)$ as a function of reduced temperature $T_R = T/T_c$ for hard-core Yukawa fluid. Legends represent the interaction range of the hard-core Yukawa fluid.

observation may be due to the difference in the critical property estimated from GC-TMMC and other methods. Furthermore, the calculation of critical point using rectilinear diameter approach is an approximate method and may lead to dubious values particularly at short interaction range, where the nature of the phase behaviour is more flat. To verify the behaviour of corresponding states of Yukawa fluid, we reserve the calculation of critical point for a future study using finite-size scaling [46], which is proven to be the precise technique. This method would certainly be more useful and perhaps necessary for short-range Yukawa fluid, where free-energy difference between two phases is found to be extremely small, which is also evident from the surface tension values listed in Table 3.

4. Conclusions

In summary, we have demonstrated grand-canonical transition-matrix Monte Carlo for the calculation of vapour–liquid coexistence and interfacial properties for a model for colloidal suspension. The method, in general, is found superior to GEMC and slab-based methods for the calculation of phase equilibria and interfacial temperature in every aspects. However, at lower temperature, slab-based method is more preferred for the calculation of interfacial properties as GCMC simulations are extremely difficult to conduct for dense liquids. Surface tension data of extremely short interaction range, $\lambda \geq 8$, is found to deviate slightly from those with $\lambda < 8$ in the corresponding plot, which may be due to the error associated with rectilinear diameter approach and scaling analysis.

Acknowledgements

This work is supported by the Department of Science and Technology (grant no. SR/S3/CE10/2006) and Department of Atomic Energy, Govt. of India (grant no. 2006/20/36/05-BRNS).

References

[1] J. Liu and E. Luijten, *Stabilization of colloidal suspensions by means of highly charged nanoparticles*, Phys. Rev. Lett. 93 (2004), 247802.
[2] V. Tohver, A. Chan, O. Sakurada, and J.A. Lewis, *Nanoparticle engineering of complex fluid behavior*, Langmuir. 17 (2001), pp. 8414–8421.
[3] R. Tuinier and C. Gogelein, *Phase behaviour of a dispersion of charge-stabilised colloidal spheres with added non-adsoring interacting polymer chains*, Eur. Phys. J. E. 27 (2008), pp. 171–184.
[4] M. Dijkstra, *Phase behavior of hard spheres with a short-range Yukawa attraction*, Phys. Rev. E. 66 (2002), 021402.
[5] S. Karanikas and A.A. Louis, *Dynamic colloidal stabilization by nanoparticle halos*, Phys. Rev. Lett. 93 (2004), 248303.
[6] C. Caccamo, G. Pellicane, and D. Costa, *Phase transitions in hard-core Yukawa fluids: Toward a theoryof phase stability in protein solutions*, J. Phys.: Condens. Matter 12 (2000), pp. A437–A442.
[7] F.W. Tavares and J.M. Prausnitz, *Analytic calculation of phase diagrams for solutions containing colloids or globular proteins*, Colloid Polym. Sci. 282 (2004), pp. 620–632.
[8] A. Fortini, A. Hynninen, and M. Dijkstra, *Gas-liquid phase separation in oppositely charged colloids: Stability and Interfacial tension*, J. Chem. Phys. 125 (2006), 094502.
[9] M. Gonzalez-Melchor, C. Tapia-Medina, L. Mier-y-Teran, and J. Alejandre, *Surface tension at the liquid–vapor interface of screened ionic mixtures*, Condens. Matter Phys. 7 (2004), pp. 767–778.
[10] T. Kristof, D. Boda, J. Liszi, D. Henderson, and E. Carlson, *Vapour–liquid equilibrium of the charged Yukawa fluid from Gibbs ensemble Monte Carlo simulations and the mean spherical approximation*, Mol. Phys. 101 (2003), pp. 1611–1616.
[11] C. Caccamo, G. Pellicane, D. Costa, D. Pini, and G. Stell, *Thermodynamically self-consistent theories of fluids interacting through short-range forces*, Phys. Rev. E. 60 (1999), pp. 5533–5543.
[12] D. Fu and J. Wu, *A self-consistent approach for modelling the interfacial properties and phase diagram of Yukawa, Lennard-Jones and square-well fluids*, Mol. Phys. 102 (2004), pp. 1479–1488.
[13] E.B. El Mendoub, J.F. Wax, and N. Jakse, *Phase diagram of the hard-core Yukawa fluid within the integral equation method*, Phys. Rev. E. 74 (2006), 052501.
[14] Y. Duda, A. Romero-Martinez, and P. Orea, *Phase diagram and surface tension of the hard-core attractive Yukawa model*

of variable range: Monte Carlo simulations, J. Chem. Phys. 126 (2007), 224510.
[15] U.F. Galicia-Pimentel, J. Lopez-Lemus, and P. Orea, *Liquid–vapor interfacial properties of attractive Yukawa fluids*, Fluid Phase Equilib. 265 (2008), pp. 205–208.
[16] B. Smit and D. Frenkel, *Vapor–liquid equilibria of the hard-core Yukawa fluid*, Mol. Phys. 74 (1991), pp. 35–39.
[17] M.H.J. Hagen and D. Frenkel, *Determination of phase diagrams for the hard-core attractive Yukawa system*, J. Chem. Phys. 101 (1994), pp. 4093–4097.
[18] E. Lomba and N.G. Almarza, *Role of the interaction range in the shaping of phase diagrams in simple fluids. The hard-sphere Yukawa fluid as a case study*, J. Chem. Phys. 100 (1994), pp. 8367–8372.
[19] K.P. Shukla, *Phase equilibria, thermodynamic properties of hard core Yukawa fluids of variable range from simulations and an analytical theory*, J. Chem. Phys. 112 (2000), pp. 10358–10367.
[20] P. Orea and Y. Duda, *On the corresponding states law of the Yukawa fluid*, J. Chem. Phys. 128 (2008), 134508.
[21] M. Gonzalez-Melchor, A. Trokhymchuk, and J. Alejandre, *Surface tension at the vapor/liquid interface in an attractive hard-core Yukawa fluid*, J. Chem. Phys. 115 (2001), pp. 3862–3872.
[22] J.K. Singh, D.A. Kofke, and J.R. Errington, *Surface tension and vapor–liquid phase coexistence of the square-well fluid*, J. Chem. Phys. 119 (2003), pp. 3405–3412.
[23] J.R. Errington, *Direct calculation of liquid–vapor phase equilibria from transition matrix Monte Carlo simulation*, J. Chem. Phys. 118 (2003), pp. 9915–9925.
[24] J.R. Errington, *Evaluating surface tension using grand-canonical transition-matrix Monte Carlo simulation and finite-size scaling*, Phys. Rev. E. 67 (2003), 012102.
[25] D.A. Kofke, *Gibbs–Duhem integration: A new method for direct evaluation of phase coexistence by molecular simulation*, Mol. Phys. 78 (1993), pp. 1331–1336.
[26] D. Moller and J. Fischer, *Vapor–liquid-equilibrium of a pure fluid from test particle method in combination with NPT molecular-dynamics simulations*, Mol. Phys. 69 (1990), pp. 463–473.
[27] A. Lofti, J. Vrabec, and J. Fischer, *Vapor–liquid equilibria of the Lennard-Jones fluid from the NPT plus test particle method*, Mol. Phys. 76 (1992), pp. 1319–1333.
[28] D. Moller, *Correction*, Mol. Phys. 75 (1992), pp. 1461.
[29] K. Binder, *Monte Carlo calculation of the surface tension for two- and three-dimensional lattice-gas models*, Phys. Rev. A. 25 (1982), pp. 1699–1709.
[30] S.K. Kwak, J.K. Singh, and J. Adhikari, *Molecular simulation study of vapor–liquid equilibrium of morse fluids*, Chem. Prod. Proc. Model. 2 (2007), 8.
[31] J.K. Singh and J.R. Errington, *Calculation of phase coexistence properties and surface tensions of* n*-alkanes with grand-canonical transition Monte Carlo simulation and finite-size scaling*, J. Phys. Chem. B. 116 (2006), pp. 1369–1376.
[32] J.K. Singh and D.A. Kofke, *Molecular simulation study of vapor–liquid interfacial behavior of a dimer-forming associationg fluid*, Mol. Simul. 30 (2004), pp. 343–351.
[33] J.K. Singh and D.A. Kofke, *Molecular simulation study of the effect of pressure on the vapor–liquid interface of square-well fluid*, Langmuir 21 (2005), pp. 4218–4226.
[34] J.K. Singh and S.K. Kwak, *Surface tension and vapor liquid phase coexistence of confined square well fluid*, J. Chem. Phys. 126 (2007), 024702.
[35] J.K. Singh, G. Sarma, and S.K. Kwak, *Thin-thick surface phase coexistence and boundary tension of the square-well fluid on a weak attractive surface*, J. Chem. Phys. 128 (2008), 044708.
[36] J.R. Errington, *Evaluating surface tension using grand-canonical transition-matrix Monte Carlo simulation and finite-size scaling*, Phys. Rev. E: Stat. Nonlin. Soft Matter Phys. 67 (2003), 012102/012101-012102/012104.
[37] B.A. Berg and T. Neuhaus, *Multicanonical ensemble: A new approach to simulation first-order phase transitions*, Phys. Rev. Lett. 61 (1992), pp. 9–12.
[38] A.M. Ferrenberg and R.H. Swendsen, *New Monte Carlo technique for studying phase transitions*, Phys. Rev. Lett. 61 (1988), pp. 2635–2638.
[39] L.J. Van Poolen, C.D. Holcomb, and V.G. Niesen, *Critical temperature and density from liquid–vapor coexistence data: Application to refrigerants R32, R124, and R152a*, Fluid Phase Equilib. 129 (1997), pp. 105–111.
[40] D. Frenkel and B. Smit, *Understanding Molecular Simulation: From Algorithms to Applications*, 2nd ed., Academic Press, New York, 2002.
[41] J.I. Siepmann and D. Frenkel, *Configurational-bias Monte Carlo: a new sampling scheme for flexible chains*, Mol. Phys. 75 (1992), pp. 59–70.
[42] J. Delhommelle, A. Boutin, B. Tavitian, A.D. Mackie, and A.H. Fuchs, *Vapour–liquid coexistence curves of the united-atom and anisotropic united-atom force fields for alkane mixtures*, Mol. Phys. 96 (1999), pp. 1517–1524.
[43] B. Chen, J.I. Siepmann, K.J. Oh, and M.L. Klein, *Aggregation–volume-bias Monte Carlo simulations of vapor–liquid nucleation barriers for Lennard-Jonesium*, J. Chem. Phys. 115 (2001), pp. 10903–10913.
[44] D. Bhatt, A.W. Jasper, N.E. Schultz, J.I. Siepmann, and D.G. Truhlar, *Critical properties of aluminum*, J. Am. Chem. Soc. 128 (2006), pp. 4224–4225.
[45] S. Wierzchowski and D.A. Kofke, *A general-purpose biasing scheme for Monte Carlo simulation of associating fluids*, J. Chem. Phys. 114 (2001), pp. 8752–8762.
[46] N.B. Wilding and A.D. Bruce, *Density fluctuations and field mixing in the critical fluid*, J. Phys.: Condens. Matter. 4 (1992), pp. 3087–3108.